Fractal Scaling in Motor Sequence Learning: Examining Acceleratory Movement Variability in a Step-based Discrete Sequence Production Test Among Fast and Slow Performers

Marcel Hildebrandt (s2763540)

Department of Psychology, University of Twente

202000384: M12 BSc Thesis PSY

Supervisor: Dr. Russell Chan

Date: 05.07.2024

Words: 11499

Abstract

This study explores the applicability of fractal analysis, specifically through Hurst exponents, in understanding motor sequence learning dynamics within a modified Discrete Sequence Production (DSP) task using a dance mat interface. The primary objective was to determine whether Hurst exponents could predict individual performance, adaptation to novel sequences, and distinguish between proficient and less proficient performers. Participants (n=22) performed sequences on the dance mat, while their Center of Mass movements were captured using motion sensors. Hurst exponents were calculated for each trial, segmented into movement preparation and sequence execution phases, to assess fractal properties of the motor output. Findings suggest that during the movement preparation phase, there is a trend of increasing and less varied Hurst exponents among better performers, which could indicate more effective anticipation and motor planning. However, in the sequence execution phase, Hurst exponents did not directly predict performance or adaptability, as consistently high Hurst exponents indicative of fractal scaling were observed among both proficient and less proficient performers. Some of the fastest participants displayed a pattern of reduced and more varied Hurst exponents compared to others during the sequence execution period. Additionally, they also demonstrated an increase in fractal properties within their acceleratory movements in response to changing task constraints in the last block of the experiment. This paper proposes that the reduction of fractal motor output may reflect a mode of sequence execution optimized for rapid and automatic execution of consolidated movement patterns with minimal cognitive control. Conversely, consistently high Hurst exponents during the sequence execution phase could indicate a performance strategy that emphasizes accuracy and exploration, involving ongoing cognitive engagement and control, regardless of the performers' speed.

Artificial Intelligence Disclaimer

Throughout this work, OpenAI's artificial Intelligence tool ChatGPT (GPT-4) was utilized to streamline statistical analysis. Specifically, it was used to help speed up the debugging process of code within R studio. Furthermore, it was used to help organize thoughts and refine paragraph structure; however, it was not used to generate substantial portions of the textual content. The core arguments, analyses, and conclusions were derived independently to maintain the originality and integrity of the academic work.

Fractal Scaling in Motor Sequence Learning: Examining Acceleratory Movement Variability in a Step-based Discrete Sequence Production Test Among Fast and Slow Performers

1. Introduction

1.1 Motor Sequence Learning and the Cognitive Framework for Sequential Motor Behaviour

Everybody who learned how to ride a manual transmission car has probably made the experience that initially, the task of shifting gears demands considerable attention and effort. However, with practice, these actions then become increasingly automatic and habitual, and the driver is able to shift gears with minimal cognitive effort. This progression of complex motor sequences becoming more automatic with repetitive practice is an example of motor sequence learning (MSL), which has long been a topic of investigation in research (Verwey, 2023). The most widely used paradigm to study MSL is the Discrete Sequence Production (DSP) task. Traditionally, this task requires participants to respond to a series of visual stimuli by pressing keys on a keyboard in a specific sequence. Each key press corresponds to one element of the sequence, allowing researchers to measure the accuracy and speed of each response. The emerging evidence from this paradigm has led to the latest iteration of the Cognitive Framework for sequential motor behavior (C-SMB 2.0) (Verwey, 2023).

The C-SMB 2.0 framework aims to explain how cognitive and motor processes work together to facilitate MSL. It proposes that our brain has separate processing units for perception (perceptual processors), decision-making (central processor), and motor execution (motor processors) (Verwey, 2023). The central processor coordinates these units by integrating sensory information from perceptual processors and directing outputs to motor processors. In the C-SMB 2.0 framework, MSL is facilitated by the development of 'central-symbolic representations,' or cognitive 'chunks,' which group individual actions into cohesive units within short-term memory. This process is reinforced by associative learning at the

perceptual, central, and motor levels, which enhances the efficiency of executing motor sequences. The seasoned driver, according to the C-SMB 2.0 framework, likely has consolidated knowledge of the motor sequences for shifting gears, stored as chunks, allowing for their execution in an almost automatic fashion.

1.2 Adaptations to the DSP task in this study

In this study, we adapted the traditional DSP task, which typically involves keypress responses to visual stimuli, to a full-body interaction format using a dance mat. This modification aims to explore MSL through more dynamic and natural activities. Participants responded to sequences not with keypresses, but by stepping on designated areas of a dance mat, adding a layer of spatial and motor complexity to the task. This approach was designed to challenge the cognitive and motor control systems more comprehensively.

1.3 Movement Variability and Complexity in MSL

When repeating an action, even if the outcome is the same, no two repetitions are ever completely identical (Stergiou & Decker, 2011). While walking for example, there are fluctuations in stride length, timing, etc. with each step (Hausdorff, 2005). In the past, these slight differences in how we perform the same task repeatedly, were often seen as noise or error - something the body tried to minimize (Davids et al., 2003; Dhawale et al., 2017). However, recent research came to view this variability not as an error, but as a fundamental feature of healthy, adaptive movement (Dhawale et al., 2017; Stergiou & Decker, 2011). According to Dhawale et al. (2017), this inherent variability reflects the motor system's active experimentation process, optimizing the discovery of the most successful way to execute a given task. This shift in understanding the role of variability aligns with the broader framework of nonlinear dynamical systems theory. In this approach, the human motor system is viewed not as a rigid input-output machine, but as a web of interconnected elements constantly undergoing self-organization (Davids et al., 2003).

Traditionally, variability has been quantified using basic statistical measures such as mean and standard deviation, which describe the average and dispersion of values around this average, respectively (Sternad, 2018). However, two time series with identical means and standard deviations can exhibit significantly different underlying complexities (Goldberger et al., 2012). Complexity can be seen as a distinct concept that describes the structure within variability; not everything that varies also displays complexity (Goldberger et al., 2012). Research has found that a certain kind of complexity within a biological system's heart rate variability or stride length variability seems to be associated with healthier and more adaptive states (Ducharme & Van Emmerik, 2018; Hausdorff, 2005; Wijnants, 2014). This complexity has also been observed with advanced skill acquisition and adaptive behavior within motor learning (Kodama et al., 2023; Nourrit-Lucas et al., 2014).

Given this background, the current study aims to use suitable statistical analysis techniques to quantify the complexity within participants' motor outputs during trials of the Dance-Step Discrete Sequence Production (DS-DSP) task. To the best of our knowledge, this approach of analyzing the complexity of motor output variability with such techniques has not been explicitly applied within an MSL paradigm. By doing so, we seek to explore whether such complexity can predict participants' ability to learn and perform in a dynamic, spatially complex task like the DS-DSP task. These insights could potentially inform and refine our current understanding of MSL by adding a dimension that has often been overlooked - the complexity within motor variability.

2. Literature Review

2.1 Movement Systems as Dynamical Systems

Dynamical systems theory views movements of biological systems as a result of a self-organizing process (Davids et al., 2003; Stergiou & Decker, 2011). This organization

arises while navigating three different types of constraints to find a stable solution for a particular movement (Sigmundsson et al. 2017; Stergiou & Decker, 2011). These three constraints arise from the moving individual, the environment, and from the task itself (Sigmundsson et al. 2017; Stergiou & Decker, 2011).

2.1.1 Stability and Energy Efficiency in Dynamical Systems

The dynamical system tends to self-organize itself and gravitate towards stable states because they represent an efficient state where the organism has minimized energy usage and surprise (Friston, 2010). These stable states, known as attractors, are not static but responsive to changes in constraints (Davids et al., 2003). This means that while a stable state is energy-efficient, the system must exert a lot of energy to transition from one attractor to another (Friston, 2010). Such transitions might be triggered by changes in the individual, the environment, or the task itself - each acting as a perturbation to the current stable state that forces the system to shift and find a new configuration (Davids et al., 2003). In the context of this study's DS-DSP task, individual constraints could include fitness or current energy levels. Environmental constraints in the DS-DSP task involve the general setup of the experiment, such as the layout and sensitivity of the dance mat. Lastly, the task constraints include the complexity of the sequences to be performed and the presence of a timed cue that signals when participants need to initiate their response. These three types of constraints effectively shape the possible configurations the system can adopt, ensuring that movements are both efficient and contextually appropriate (Davids et al., 2003).

2.1.2 Exploratory Nature of Movement Variability

Dynamical systems theory views movement variability not as noise, but as a means of exploration that leads to the discovery and refinement of movement solutions within any given constraints (Dhawale et al., 2017). An analogy to this process can be found in the role natural selection plays in evolution. Just as natural selection favors variations that better fit

environmental constraints, motor learning involves exploring variations, with more successful patterns becoming more likely to persist (Dhawale et al., 2017).

2.2 Balancing Stability and Flexibility in Motor System Variability

Once a motor system has explored and identified an efficient movement strategy within a given set of constraints, it generally reduces trial-to-trial variability in movements, known as the exploitation phase (Shmuelof et al., 2012). While these attractors represent relatively stable states with reduced variability between trials, no two repetitions of the same task will ever be identical (Newell & Vaillancourt, 2001). The motor system remains inherently flexible to allow for adaptive responses to changing conditions (Wilson et al., 2008). This inherent flexibility underscores the necessity for the motor system to find a balance between too little and too much variability (Stergiou & Decker, 2011). Excessive rigidity, or too little variability, may lead to a system that is overly deterministic and unable to adapt to new or changing conditions. On the other hand, excessive variability can lead to unstable and inefficient movement patterns. Thus, maintaining an optimal level of variability is crucial for enabling both stable performance under familiar conditions and flexible adaptation to new challenges (Stergiou & Decker, 2011; Wilson et al., 2008).

2.3 Fractal Scaling: Self-Similarity and Scale-Invariance

A widely observed characteristic across various natural phenomena and biological systems, including human motor activity, is fractal scaling (Wijnants, 2014). Fractal scaling is a certain kind of complex variability that effectively balances randomness and orderliness, and is often associated as a marker of healthy and adaptive systems (Goldberger et al., 2012; Wijnants, 2014). This phenomenon exhibits two fascinating characteristics known as self-similarity and scale-invariance (Diniz et al., 2011; Stergiou & Decker., 2011; Wijnants, 2014). These characteristics can be observed in the branching structure of a tree: the overall shape is made up of smaller branches, which themselves have even tinier branches. This

'nesting' of similar forms and patterns at different scales is the essence of self-similarity and scale-invariance (Wijnants, 2014). In the example of the tree, this would be called geometric self-similarity (Ducharme & Van Emmerik, 2018). Alternatively, a process can have statistical self-similarity, where smaller segments resemble the larger pattern in their statistical properties. In human movement, this can be seen in how the fluctuations of our stride intervals over short time periods have a similar structure to how they fluctuate over longer periods for example (Hausdorff, 2005).

2.4 Quantifying Fractal Scaling with the Hurst Exponent

The Hurst exponent can be used to quantify the degree of fractal scaling within variability (Likens et al., 2023). It is a measure of persistence and long-term memory within the fluctuations of a given time series (e.g. a biological signal), and is often described as capturing long-range correlations. It assesses how strongly past values of a time series influence future values, indicating the presence of repeating patterns at different scales. A Hurst exponent close to 1 signifies that a time series exhibits fractal scaling, where fluctuations are scale-invariant and self-similar. Conversely, a Hurst exponent around 0.5 denotes a completely random and uncorrelated series of fluctuations (Likens et al., 2023). When the term 'fractal scaling' is mentioned hereafter, it refers specifically to time series where the Hurst exponent is approximately 1, highlighting a pronounced presence of these complex, self-organizing properties. Other terms that are often used to describe fractal scaling are '1/f scaling', '1/f noise', or 'pink noise' (Diniz et al., 2011; Wijnants, 2014).

2.5 Fractal Scaling in Health and Disease

Studies have found fractal properties embedded within numerous healthy biological processes. For example, healthy hearts exhibit fractal patterns in the slight variations between heartbeats, and deviations from these patterns are indicative of potential cardiac dysfunction (Ducharme & Van Emmerik, 2018; Wijnants, 2014). Similarly, in human motor systems, the

presence of fractal properties in postural sway or gait intervals is most pronounced in young, healthy individuals. These properties diminish in older adults and those with Parkinson's disease, reflecting a loss of this complex variability (Ducharme & Van Emmerik, 2018; Wijnants, 2014). Furthermore, in elderly populations, the presence of fractal properties in sway as well as gait has been shown to successfully distinguish between fallers and non-fallers (Wijnants, 2014; Zhou et al., 2017).

2.6 Implications of Fractal Scaling for Motor Learning and Adaptation

While fractal scaling is often connected to systems that balance stability with adaptability, not all out movement naturally demonstrates this fractal nature. For example, while young individuals walking at their preferred speed often have scaling exponents around 0.75, walking faster or slower results in exponents closer to fractal scaling (Ducharme & Van Emmerik, 2018). This likely stems from the fact that "constant enactment of control" or a certain kind of "intentionality" during the performance of a task seems to be necessary for the fractal properties to emerge (Diniz et al., 2011; Likens et al., 2015). In a study by Likens et al. (2015), participants performed a steering task on both a straight and a circular track. Interestingly, only the data from steering on the circular track, which demanded more constant control and more granular adjustment of the steering angle throughout the task, exhibited stronger fractal properties. They concluded that continual control seems necessary for the emergence of fractal properties in movement variability (Likens et al., 2015). Furthermore, the strength of fractal properties depends on the nature of the task itself. When tasks demand internal control and offer fewer external constraints, fractal scaling tends to be stronger (Likens et al., 2015).

In contrast, tasks that are heavily constrained by environmental factors (like tapping to a metronome) or by task constraints that limit goal-relevant behaviors can suppress the system's inherent fractal fluctuations (Likens et al., 2015; Wijnants, 2014). This is further

supported by a study from Wijnants et al. (2009), in which they examined a precision-aiming task where participants had to move a stylus quickly and accurately between small targets using their non-dominant hand. Interestingly, the fractal properties in their movement variability became increasingly visible as participants gained skill in this task, where the goal-relevant movement was highly constrained by external factors (the very small targets) as well as individual/task constraints (having to use the non-dominant hand) (Wijnants et al., 2009). This suggests that even under constraint, the emergence of stronger fractal patterns in movement variability might reflect a process of motor learning and optimization.

Moreover, a recent study by Kodama et al. (2023) found that expert slackliners, unlike novices, exhibit fractal dynamics in center of mass (COIM) accelerations during single-leg standing, indicative of more adaptive behavior required for balance. This evidence supports that fractal scaling can emerge in tasks demanding high levels of active control and adaptability.

Another study by Ducharme & Van Emmerik (2018) investigated whether fractal dynamics in gait directly reflect how well a person can adapt their movement to changing environmental constraints. They measured the fractal scaling in gait of participants during unperturbed walking at their preferred walking speeds, and then again during a split-belt treadmill task where the belts moved at different speeds, forcing participants to adapt their walking pattern. Interestingly, individuals' fractal scaling during normal walking did not predict their success on the adaptive task. However, when they faced the split-belt treadmill challenge, those who were best able to adjust their gait showed scaling exponents closer to fractal scaling (Ducharme & Van Emmerik, 2018). This suggests that fractal scaling within human motor output could emerge specifically when active control is needed to navigate a novel situation, rather than reflecting a general, pre-existing trait linked to adaptability.

2.6 Research Questions and Hypotheses for the application of Fractal Analysis within the DS-DSP Task

The preceding sections outlined the current understanding of how fractal scaling emerges within motor signals during the process of motor learning. To date, fractal analysis has not been applied specifically within a MSL task. This study aims to fill this gap by exploring how fractal analysis might add to our understanding of MSL.

2.6.1 Segmented Nature of the DS-DSP task

In this study, the DS-DSP task is structured across 10 blocks, each consisting of 48 trials. During the first nine blocks, participants practice two predetermined sequences in random order. In contrast, Block 10 introduces two new, unfamiliar sequences to assess adaptability, presenting a novel challenge and testing the transferability of learned skills. Most studies using fractal analysis have analyzed trial-by-trial variability in continuous time series spanning multiple repetitions of a task. The DS-DSP task however is inherently segmented due to its trial structure. Each trial initiates with the display of a sequence that participants must replicate, followed by a waiting period before the next sequence is displayed, which effectively segments the task into separate phases. This study will focus on the within-trial fluctuations of COM acceleration measures along the X, Y, and Z axes, captured by a portable motion capture system. The segmented nature of the DS-DSP tasks design will allow us to explore this variability during the two phases of each trial: the movement preparation phase and the sequence execution phase. This approach represents an exploratory investigation into whether such within-trial variability can yield informative insights about MSL.

2.6.2 Research Questions

The main research questions this study is trying to address are: Can the Hurst exponents obtained from the COM acceleration data predict individual performance in terms

of total trial response time? Can the Hurst exponents provide insight into how well participants adapt to the new and unfamiliar sequences in Block 10? And lastly: Are the Hurst exponents able to differentiate fast performers from slow performers within the DS-DSP task?

2.6.3 Hypotheses

We hypothesize that the fractal properties, as quantified by Hurst exponents, will become more pronounced over the course of the experiment in both the sequence execution and movement preparation periods during the DS-DSP task. This hypothesis is informed by findings from Wijnants et al. (2009), which observed stronger fractal properties in participants' movements with increased practice in a precision aiming task. Additionally, the study by Zhou et al. (2017), which found that fractal scaling in standing postural sway can successfully distinguish between fallers and non-fallers among the elderly, underlies our expectation that Hurst exponents might also increase in the movement preparation period.

Furthermore, drawing from the research by Ducharme & Van Emmerik (2018), which found that participants who adapted best to changing task constraints exhibited the highest scaling exponents, our second hypothesis posits that those who most effectively adjust to new and unfamiliar sequences will demonstrate higher Hurst exponents compared to those who perform less well under these changing task constraints. Further support for this hypothesis comes from Kodama et al. (2023), who found that expert slackliners, unlike novices, exhibit clearer fractal dynamics in COM acceleratory movements. This suggests that similar fractal properties might be indicative of better adaptation in our DS-DSP task.

3. Methods

3.1 Participants

The final sample used for analysis consisted of 22 participants (16 females, 6 males, average age 20.64 ± 2.48 years). Initially, the study included more participants; however, seven participants were excluded from the final analysis due to issues identified during data preprocessing. These exclusions and their justifications are detailed later on in the Data Preprocessing section. The participants were recruited from the university community at University of Twente in the Netherlands where the participants received credits that they needed to complete their program in exchange for participating in the study. All participants were free from any neurological, psychological, or psychiatric conditions. The study was approved by the ethics committee at the University of Twente under the request number: 210390. Furthermore, all participants provided informed consent before participating in the study.

3.2 Materials

3.2.1 Stimulus Presentation and Response Recording

The stimuli in this study were presented using the software E-Prime®. To capture the participants response times, we used a high-performance dance mat (Nonslip Dance Pad Version 5 from D-Force), which had four areas for input (↑, ↓, ←, and →) as well as a central neutral location. A 77 inch screen was positioned approximately 1.20 meters away from the center of the dance mat where the participants were standing. To process the participants inputs captured by the dance mat, we used the software JoyToKey, which enabled us to map specific keyboard inputs (W, S, D, and A) to corresponding movements on the dance mat (↑, ↓, ←, and →). This essentially translated the directional inputs of the dance mat into key presses on a traditional keyboard layout to be recognised by E-Prime®.

3.2.2 Motion Capture System

To collect kinematic data related to the COM movement of the participants, we deployed a system consisting of seven motion capture sensors from Xsens (MTw Awinda). In

order to gather accurate kinematics data for lower body movement and COM, a minimum of seven motion capture sensors were required. The system recorded the data at a rate of 100 Hz and processed it through an MTw Awinda base station, which received the data wirelessly from the sensors. Crucially, the MVN Analyze program was run on a separate computer from the stimulus presentation software to ensure uninterrupted data capture and analysis. Network latency, response delay, and event marker reception lag were all within acceptable ranges for local User Datagram Protocol (UDP) communications.

3.3 Procedure of the DS-DSP task

3.3.1 Participant Preparation with Xsens

To begin, participants received a comprehensive overview of the study's purpose and their right to stop participation at any given moment. After removing their shoes, participants were asked to provide consent for the physical contact that was necessary to place the Xsens sensors on their body. The seven Xsens sensors were securely fastened to participants' feet, calves, thighs, and pelvis using Velcro straps.

3.3.2 Xsens Calibration

To start Xsens sensor calibration, participants were instructed to stand still with their arms relaxed by their sides. Once the researcher has initiated the calibration process, the participant then proceeded to walk along a straight line up until a marking on the ground, which was a distance of around four meters. The participant then needed to turn around and walk back towards the initial starting position. The MVN Analyze software then used this data to process the calibration. If the software did not indicate a successful calibration, participants had to repeat the procedure.

3.3.3 Executing the DS-DSP task with Xsens

After the sensor calibration was finished, the participants received detailed instructions on the experiment's procedure. This included an explanation of the number of

Blocks, Trials and the frequency and length of breaks during the experiment. The necessity of stepping with the entire foot, rather than just the toes, was emphasized. Participants were instructed to perform the sequences quickly and accurately in a way that felt natural and comfortable. Lastly, participants were informed to begin the sequence only when the Go Signal was displayed and to avoid execution when the NoGo Signal was presented.

When ready, participants positioned themselves at the center of the dance mat facing the screen. Then, the recording for the Xsens data was started followed by the initiation of the script in E-Prime®. To start the stimulus presentation, participants pressed their foot on the X panel at the dance mat's top left corner, which corresponded to the spacebar in the JoyToKey setup. Once running, E-Prime® then recorded the response times and accuracy of the participants' steps.

The task was presented through a series of visual stimuli on the screen. Each trial consisted of six sequential events, starting with a default screen displaying a yellow cross for 1000 ms. This was followed by the appearance of six rectangular placeholders in yellow, each visible for 75 ms. After displaying the sequence, the screen returned to the default view, and a 1500 ms pause followed to allow participants to prepare for their movement. After the pause, either a blue (Go) or red (NoGo) cross appeared in the middle of the screen. For the Go stimuli, participants then needed to perform the previously displayed sequence by reproducing the steps on the four input areas of the dance mat that corresponded to the six rectangular yellow placeholders they had seen in sequential fashion. If they moved too early, a message indicating 'Too early!' appeared, halting the trial. For NoGo stimuli, the waiting time lasted 3 seconds until the next sequence was displayed. After the six steps, feedback was provided, highlighting any errors made during the sequence. Correct responses earned a message indicating "Good" work before the next trial began. Figure 1 illustrates the

experimental setup, including the dance mat interface and the sequence of visual cues presented to the participants.

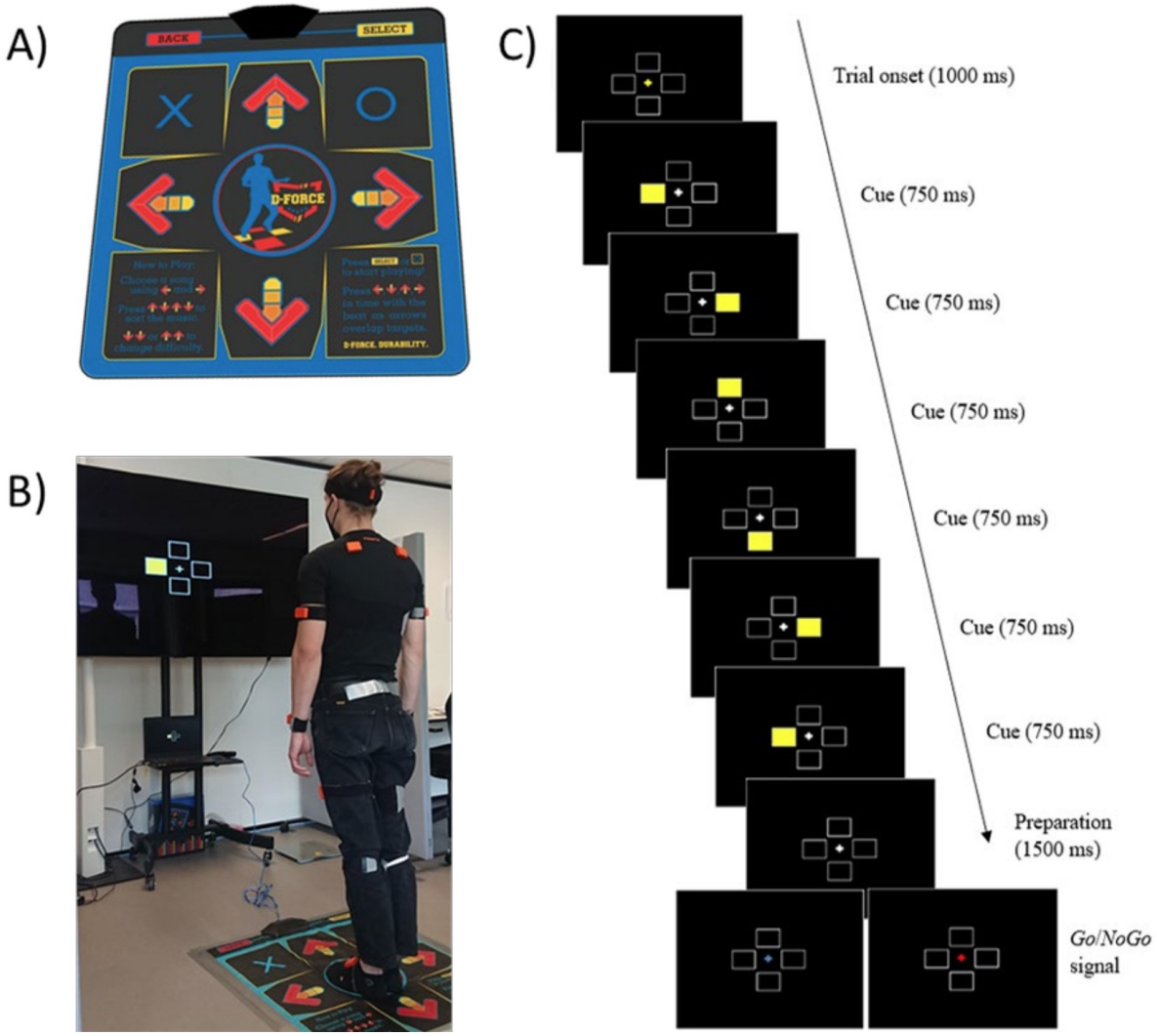

Fig. 1. Experiment design and sequence of visual cues. A) Dance mat used for the experiment. B) Participant ready at the experimental setup. C) Detailed sequence of visual cues and their timing used during the trials. This figure was taken from Chan et al. (2022), licensed under CC BY 4.0: https://doi.org/10.31234/osf.io/ypt7n

Furthermore, the E-Prime® script was also designed to send event markers to MVN Analyze via a User Datagram Protocol (UDP) using a switch/router setup. These event markers enrich the motion capture data by indexing each instance a stimulus is presented,

such as the display of sequence stimuli or feedback screens, the Go or NoGo signals, and the precise moments when a participant executed one of the six steps within a sequence.

3.3.4 Experiment Structure

The experiment was designed to include 10 blocks in total: the first 8 blocks served as learning blocks, while the last 2 blocks were test blocks. Each Block consisted of 48 Trials and 4 NoGo Trials. During the learning blocks (1-8), participants practiced two sequences (24 Trials per sequence) in random alternating fashion. These sequences remained the same throughout the learning blocks. Block 9 served as a comparison block, where participants continued to practice the same two familiar sequences. In contrast, Block 10 introduced two new, unfamiliar sequences that participants had not practiced before. The goal was to assess how the skill learned on the initial sequences transferred to the unfamiliar sequences in Block 10. The sequences received by participants were counterbalanced across individuals, ensuring that each participant encountered the same sequences but initiated from different starting positions. A key difference between this Dance-Step DSP task and the traditional DSP task is the limited number of effectors (two feet) available to participants. This allowed them to find their own natural approach to performing the sequences using any combination of their two feet on the dance mat. After finishing each block, participants received a completion notice ('This is the end of the session.'), along with a summary of their results, including average response time and error percentage.

Participants were offered structured breaks to prevent physical and mental fatigue, including 3-minute rests between blocks and a longer 10-minute break after Block 4. Additionally, within each block, participants had a 30-second break halfway through. The physical demand and effort of participants were consistently evaluated using the NASA-TLX scale during the breaks after each Block (Hart & Staveland, 1988). In total, participants performed 480 Trials, 384 over the eight learning blocks and 96 over the two test blocks.

3.4 Data Analysis

3.4.1 Data Preprocessing

After completing the data collection phase, the E-Prime® script provided behavioral data, capturing the response time (RT) and accuracy for each step within a trial as recorded by inputs on the dance mat. The dataset was then filtered to retain only the relevant columns and rows, focusing on the essential variables: 'Subject', 'Block', 'Trial', 'Step', 'Sequence' (coded as 1 or 2, representing the two different sequences practiced within a trial), 'Step.ACC' (coded as 0 for incorrect steps and 1 for correct steps), and RT. Additionally, a new variable, 'Trial.ACC', was added, which was coded as 1 for trials where every step was performed correctly, and 0 if any of the steps was incorrect.

Furthermore, the seven motion capture sensors provided a dataset of the lower body kinematics during the experiment. This dataset included variables such as position, velocity, and acceleration for each of the X, Y, and Z axes of each sensor. In addition to that, it also included aggregated metrics from all seven sensors representing the COM displacement, velocity, and acceleration. For methodological simplicity and to enhance sensitivity to changes in movement, the analysis was narrowed down to the acceleration variables of the COM in the X, Y, and Z dimensions. Acceleration was chosen as it is a derivative of velocity, making it a more sensitive measure of changes in movement dynamics. Here, the participant with the identifier 21 was excluded because the motion capture data for that participant was missing.

To further prepare the Xsens data for subsequent analysis, the next step involved segmenting the motion capture recording into individual time series for each trial of every participant. The first step here was to identify each 'Go' signal that was sent, and added to the Xsens recording by the E-Prime® script via UDP. Since each participant performed 480 trials in total across the ten blocks, there should also have been 480 'Go' signals within the data.

However, the participants with the identifiers 7, 8, 17, and 29 had some of those markers missing, likely due to transmission losses in the UDP signaling, and therefore were also excluded from further analyses. The identified 'Go' signals then marked the beginning of each trial within the motion capture recording of each participant. The next step was to identify all rows of data that correspond to the movement preparation phase prior to the 'Go' signal of each trial, and all rows belonging to the sequence execution phase following each 'Go' signal. The easier part of the two was the movement preparation phase, as it spanned from the display of the last stimulus until the 'Go' signal was displayed. This interval was set to 1.5s in the E-Prime® script. Given the sampling rate of 100Hz by the Xsens sensors, that interval of 1.5s corresponded to 150 rows of data within the motion capture data. Therefore, these 150 rows prior to each 'Go' signal were defined as the time series for each trial's movement preparation period.

For the sequence execution period, the approach involved segmenting the data starting from each 'Go' signal of a trial up to the last occurring step marker before the subsequent 'Go' signal. At this stage, the participants with the identifier 33 and 18 were excluded. The sequence execution data for participant 33 were incomplete in two trials due to interruptions in the Xsens recording during the experiment. For participant 18, the step markers were missing in block 10, likely due to an error in the setup of the E-Prime® script for that block. Unlike the movement preparation period, the sequence execution time series varied in length across trials and between participants. To avoid introducing a confounding variable related to the variability in time series length, since the accuracy of Hurst exponent estimation improves with longer time series, we standardized the data to a fixed length (Likens et al., 2023). This length corresponds to the shortest trial in the dataset, which was 135 rows. Given that the trials from this particular participant were significantly shorter on average than those of most other participants, an additional 65 rows were included beyond each last occurring step

marker. This adjustment extended the fixed time window to a consistent length of 200 rows across all trials for subsequent analysis. For some of the shorter trials, this extension then also captured some of the data in the recording after the last occurring step marker. These data points however, were still expected to be informative as they capture movements related to stabilizing and rebalancing after the final step. The approach of using a fixed portion of each trial was validated by computing the Hurst exponent for both the fixed time window and the full trial length of selected trials and blocks, as described in the following section. The results showed close alignment overall, reinforcing the validity of using a fixed time window for fractal analysis in our study. Additionally, using a fixed time window of 200 rows per trial also significantly reduced the computational demands associated with calculating the Hurst exponent. A visual representation of the time series data for both the movement preparation phase and the sequence execution phase, along with the fixed time window approach, is depicted in Figure 2.

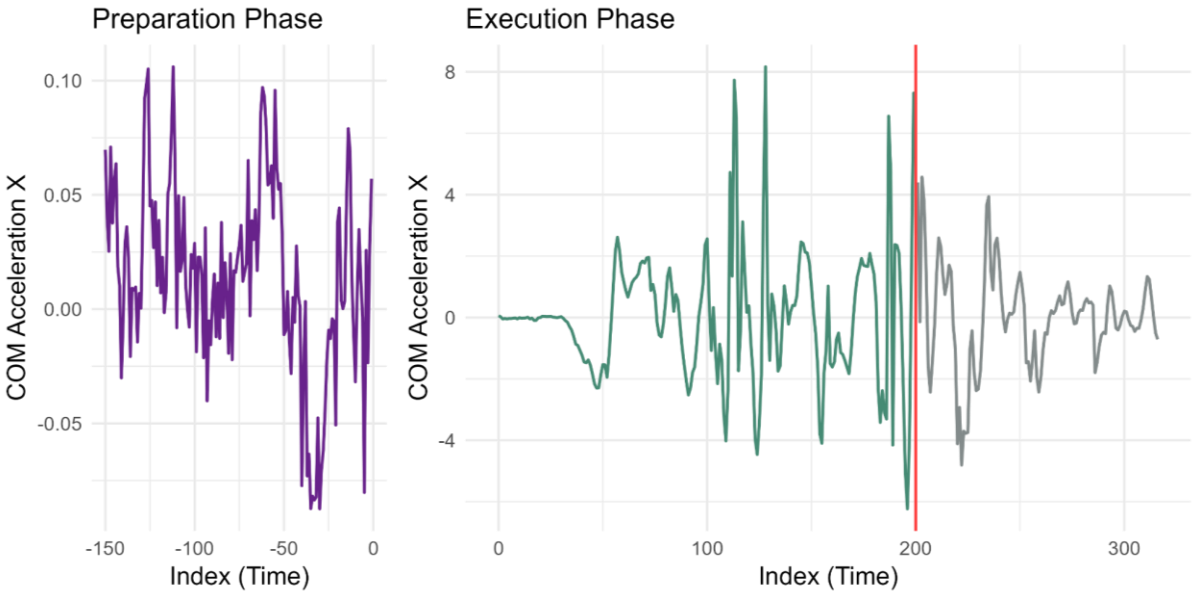

Fig. 2. Time Series Representation of Movement Preparation and Execution Phase for Trial 5, Block 5 of Participant 15. The red line in the execution phase time series represents the cutoff at 200 data points, which was used as a standardized time window for analysis.

3.4.3 Obtaining Hurst Exponents

The Hurst exponents were calculated to assess the fractal scaling properties of the time series data from the DS-DSP task. Traditionally, Detrended Fluctuation Analysis (DFA) has been the most widely used method for estimating fractal scaling in time series data (Likens et al., 2023). However, DFA typically requires a minimum of around 500 data points to accurately capture the underlying scaling exponents within the data. To address the limitation of our time series being shorter, we used another estimation method called the Hurst-Kolmogorov (HK) method as described in Likens et al. (2023). The HK method allows for estimation of Hurst exponents with time series as short as 64 data points and usually outperforms DFA (Likens et al., 2023).

To compute the Hurst exponents, we utilized the 'inferH()' function from the 'HKprocess' package in R. This function implements a Bayesian accept-reject sampling algorithm to estimate the Hurst exponent (Likens et al., 2023). This function takes as an argument the number of samples (n) to be drawn from the posterior distribution of H. Following the recommendations of Mangalam et al. (2023), the sample size of n was set to 50 in order to balance computational demand with accuracy of the estimation. Consistent with Likens et al. (2023), we took the median of the resulting sample as the estimate of the Hurst exponent for each trial's time series.

To further enhance computational efficiency, parallel processing was used through the R package 'parallel'. This approach aimed to overcome the limitations of R's default single-threaded operation, which can restrict the processing speed for extensive computations like Hurst exponent estimations. A cluster of worker nodes was set up using available cores on the machine, reserving one core for system processes. Necessary libraries and functions for calculating Hurst exponents were loaded onto each worker node. The dataset was divided into

manageable chunks, and Hurst exponents for each chunk were calculated across multiple cores to reduce overall computational time.

Following the calculation of Hurst exponents, the results were merged into two dataframes: one for the movement preparation phase and another for the sequence execution phase. Next, the behavioral data captured through the dance mat via E-Prime®, which included trial accuracy and response times for each step, was prepared for integration. To the Hurst exponent dataframes, we added three variables from the behavioral data: trial_mean_rt (the average response time for each of the six steps within a trial), trial_total_rt (the total duration in milliseconds to complete the trial), and trial_acc (a binary indicator of trial accuracy, where '1' represents accurate and '0' represents inaccurate trials). This merging process yielded two comprehensive data frames that were utilized for subsequent analyses. These final datasets comprised the following variables for each trial of every participant: 'Subject', 'Block', 'Trial', 'Sequence', 'hurst_acceleration_x', 'hurst_acceleration_y', 'hurst_acceleration_z', 'trial_mean_rt', 'trial_total_rt', and 'trial_acc'."

3.4.4 Data Analysis across Participants

To demonstrate learning effects within the experiment, we analyzed response times and step accuracies from the behavioral data using linear mixed-effects models (LMM) and logistic generalized mixed-effects models, respectively. Both models included 'Block' as a fixed effect with ten levels corresponding to each of the ten blocks of the experiment, to examine changes over the course of the experiment, and 'Subject' as a random effect to account for individual variations in performance. An ANOVA, using Type II Wald chi-square tests, was performed on each mixed model to assess significant variations in response times and step accuracies across different blocks. Additionally, post hoc pairwise comparisons between blocks were conducted to precisely identify at which stages participants on average demonstrated significant improvements. Prior to this analysis, we applied a

filtering criterion to exclude trials where response times were more than 2.5 standard deviations above the block mean of each individual. This resulted in one or two Trials being removed per participant per block on average. This step was necessary to remove data from trials where participants did not trigger a response on the dance mat accurately, leading to inflated response times due to delayed recognition of the input error that could obscure the results.

The statistical analysis for the Hurst exponents of both the movement preparation period and the sequence execution period followed a similar structure. We first employed LMM's to determine whether the Hurst exponents varied significantly across different blocks of the experiment, indicating changes in fractal scaling as participants progressed through the blocks. These models specified 'Block' as a fixed effect with ten levels and both 'Subject' and 'Trial' as random effects to account for intra-subject variability and the repeated measures across trials. After fitting the models, we conducted an ANOVA with Type II Wald chi-square tests to evaluate if significant differences existed in the Hurst exponents across the blocks. The significance of the block effect would indicate differences in fractal scaling at various stages of the experiment across all participants. To further explore where these changes occurred, post hoc comparisons were conducted. These comparisons helped identify specific blocks within the experiment between which significant changes in Hurst exponents emerged.

3.4.5 Data Analysis focused on Fast vs. Slow Participants

Following the broad analysis of changes in Hurst exponents across blocks, the next phase of the analysis focused on individual differences in adaptation to task demands by categorizing participants into two performance-based groups. To explore adaptive responses to new and unfamiliar sequences introduced in Block 10, participants were ranked based on their performance in accurately completed trials only, specifically measured by the total trial

response time (trial_total_rt) for these trials. Focusing on response times in only accurate trials ensured that the selected participant could perform the new unfamiliar sequences both fast and accurately as a measure of adaptability. The three fastest participants were classified as 'Fast' performers, representing those who adapted most effectively to the new sequences. Conversely, the three slowest participants were identified as 'Slow' performers, indicating a less effective adaptation.

For each group, the 'Fast' and 'Slow' performers, further analyses were conducted to examine changes in Hurst exponents across three specific blocks: the initial exposure (Block 1), after extended practice of the initial sequences (Block 9), and during the introduction of new sequences (Block 10). The aim was to assess whether the Hurst exponents could distinguish between effective and less effective performers. To achieve this, LMM's were fitted for each axis of the Hurst exponents, for both the movement preparation phase and the sequence execution phase. The models were specified to include fixed effects for the group (‘Fast’ vs. ‘Slow’) and random effects for individual subjects. Each model was analyzed using ANOVA to test if the mean Hurst exponents for the 'Fast' and 'Slow' groups differed significantly at any of the three specified blocks during the experiment.

4. Results

4.1 Changes in Response Times and Step Accuracies Across Blocks and Participants

The type II Wald chi-square test from the linear mixed-effects model for RT showed a significant effect of Block, $\chi^2(9) = 2098.6$, $p < .001$. The post-hoc pairwise comparison revealed that the mean RT across participants in Block 2 was 328ms faster than in Block 1 (SE = 11.8, $p < .001$). Furthermore, there was a significant shift in RTs from Block 9 to Block 10, with RTs in Block 10 being 76ms slower on average compared to Block 9 (SE = 11.8, $p < .001$). Similarly, type II Wald chi-square test from the logistic generalized mixed-

effects model for step accuracies also indicated a significant effect of Block, $\chi^2(9) = 650.3$, $p < .001$. Accompanying the significant decrease in RT from Block 1 to Block 2 within the RT model, the pairwise post hoc comparisons within the step accuracy model revealed that this was complemented by an improvement of step accuracy in Block 2 compared to Block 1. Specifically, the log odds of executing an accurate step were 1.09 units higher in Block 2 than in Block 1 (SE = 0.07, $p < .001$). Secondly, another significant shift occurred in the comparison of Block 9 and Block 10, where the log odds of performing an accurate step in Block 10 were 0.5 units lower compared to Block 9 (SE = 0.07, $p < .001$). The estimated means across the blocks of both the step accuracy and RT model are illustrated in Figure 3.

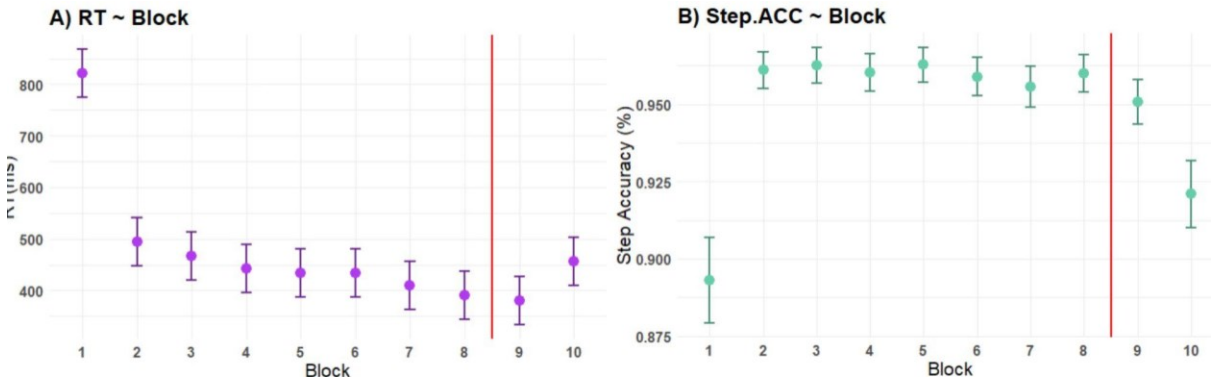

Fig. 3. Learning effects over experimental blocks. A) Estimated means and 95% confidence intervals of response times across blocks. B) Estimated means and 95% confidence intervals of step accuracy across blocks and participants. The red line in both plots between Blocks 8 and 9 indicates the transition to test blocks.

4.2 Changes in Hurst Exponents Across Blocks and Participants

4.2.1 Movement Preparation Period

The Type II Wald chi-square tests from the linear mixed-effects models assessing Hurst exponents during the movement preparation period across the three axes of acceleration demonstrated significant effects of block on the Hurst exponents for all axes (Hurst

Acceleration X: $\chi^2(9) = 85.157$, $p < .001$; Hurst Acceleration Y: $\chi^2(9) = 77.683$, $p < .001$; Hurst Acceleration Z: $\chi^2(9) = 54.696$, $p < .001$). Post hoc comparisons of the Acceleration X model revealed that there was a long term increase in Hurst exponents beginning from Block 7, with Hurst exponents in Block 7 estimated to be higher by .022 compared to Block 1 (SE = 0.005, $p < .001$). This pattern of the Hurst exponent's increase being significant continued through Blocks 8, 9, and 10, when compared to Block 1. Similarly, the Acceleration Y model also showed a significant increase starting from Block 7, with Hurst exponents in Block 7 being higher by .018 compared to Block 1 (SE = 0.006, $p = .035$). This increase remained significant in Block 8 and Block 10, in contrast with Block 1. For the Acceleration Z model, the first significant increase was observed in the contrast of Block 2 and Block 8, with Hurst exponents in Block 8 being higher by .028 compared to Block 2 (SE = 0.0064, $p < .001$). Another significant increase was also observed in Block 10, with Hurst exponents in Block 10 being higher by .026 compared to Block 2 (SE = 0.006, $p = .002$).

4.2.2 Sequence Execution Period

For the sequence execution period, the Type II Wald chi-square tests for Hurst exponents similarly exhibited significant effects of block for all three axes of acceleration (Hurst Acceleration X: $\chi^2(9) = 316.73$, $p < .001$; Hurst Acceleration Y: $\chi^2(9) = 170.86$, $p < .001$; Hurst Acceleration Z: $\chi^2(9) = 26.039$, $p < .001$). Post hoc comparisons of the Acceleration X model revealed a pattern of gradual decrease in Hurst exponents, beginning as early as Block 1 compared to Block 3, with a decrease of .015 (SE = 0.003, $p < .001$). This decreasing trend continued from Block 3 to Block 4 by .012 (SE = 0.003, $p = .003$) and from Block 4 to Block 10 by .012 (SE = 0.003, $p = .003$), indicating a long-term decline in the Hurst exponents of acceleratory movements in the X axis as participants progressed through the blocks. For the Acceleration Y model, the first significant decrease appeared between Block 1 and Block 5, with a reduction of .01 in Hurst exponents (SE = 0.003, $p = .012$). A

similar reduction occurred from Block 5 to Block 7 by .01 (SE = 0.003, p = .014), with the contrasts between Block 5 and Block 8, and 9 remaining to be significant. Lastly, the Acceleration Z model presented a much narrower range of estimated mean Hurst exponents across participants, fluctuating between approximately .99 and .995. The first notable change was a significant decrease from Block 2 to Block 5 by -.004 (SE = 0.001, p = .013). The estimated means of Hurst exponents across blocks for all three axes during both the movement preparation period and the sequence execution period can be seen in Figure 4.

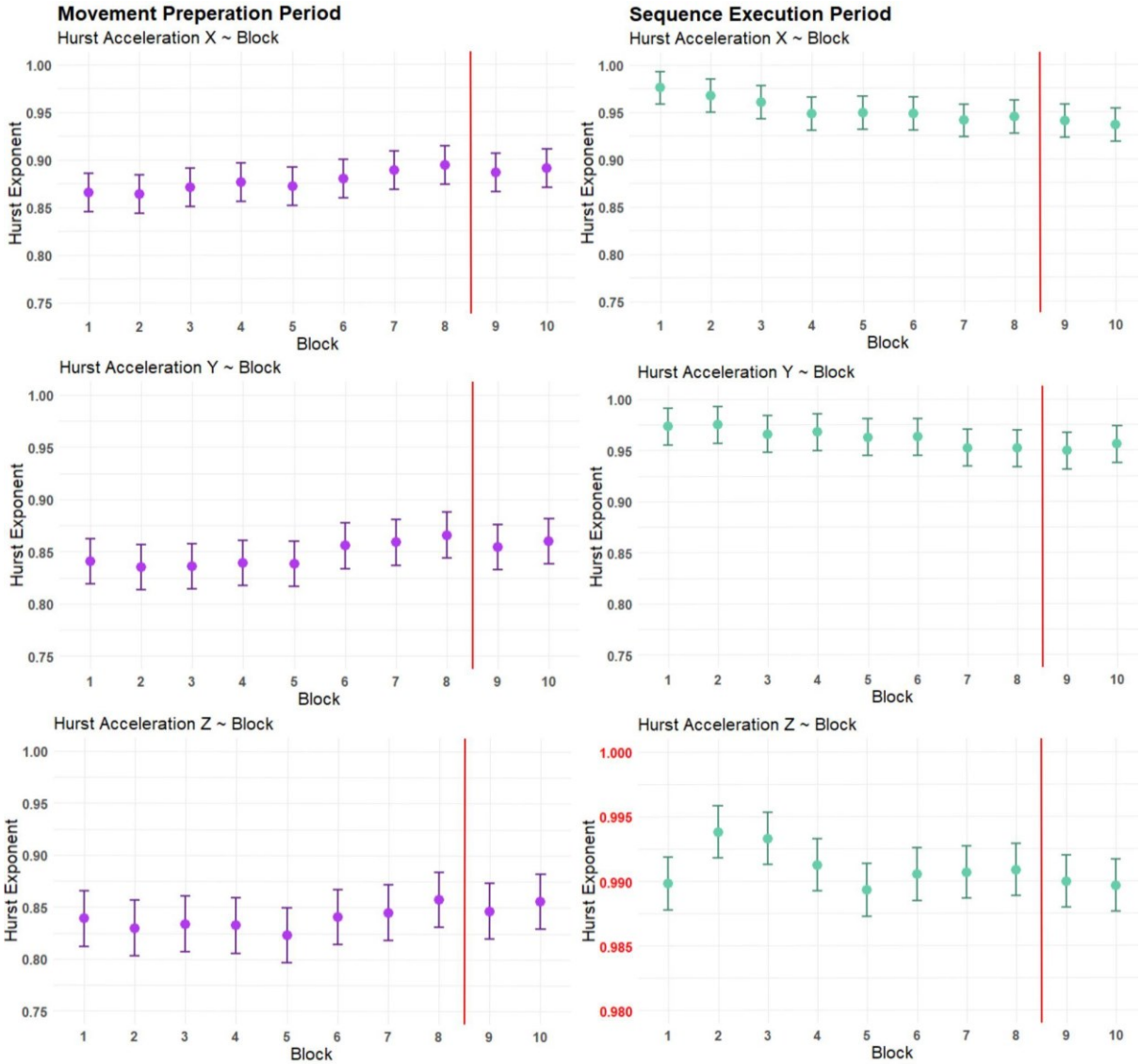

Fig. 4. Changes in Hurst exponents across blocks for the three axes of acceleration during Movement preparation and execution periods. The left side of the figure displays the

estimated means of Hurst exponents across the axes of acceleration during the movement preparation phase, while the right side presents these measures during the sequence execution phase. Error bars represent the 95% confidence intervals of the estimated means. The red vertical lines within the plots indicate the transition to the testing phase within the experiment. Additionally, the Y-scale of the plot for Hurst Acceleration Z during the sequence execution phase is highlighted in red to emphasize the adjusted scale, ensuring that differences in means and confidence intervals are visually distinguishable.

4.3 Differences in Hurst Exponents across Fast vs. Slow Performers

This next segment of the analysis focused on individual differences regarding the Hurst exponents and their potential implications for MSL and adaptability to new task demands. Figure 5 presents the mean total response times for the three fastest (Participant 6, 15, and 28) and the three slowest (26, 23, 35) participants in accurately performed trials in Block 10, who were chosen as the subjects of analysis for the upcoming results.

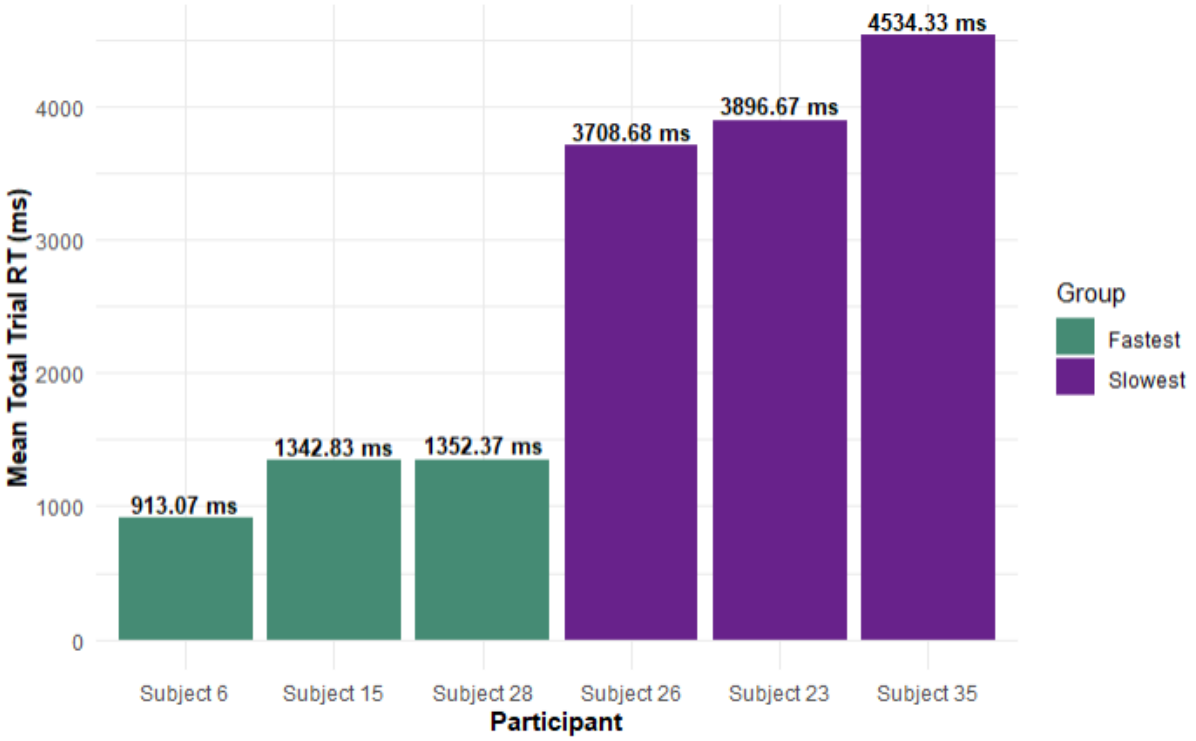

Fig. 5. Mean total trial RTs for the fastest and slowest participants in block 10.

4.3.1 Movement Preparation Period

In Block 1 of the movement preparation period, the ANOVA did not reveal any significant differences in Hurst exponents between performers belonging to the 'Fast' and 'Slow' groups across the x, y, or z axes. However, in Block 9, there were significant group differences in Hurst exponents for all three axes (Hurst Acceleration X: $F(1, 4) = 8.62$, $p = .043$; Hurst Acceleration Y: $F(1, 4) = 16.30$, $p = .015$; and Hurst Acceleration Z: $F(1, 4) = 8.89$, $p = .041$). These differences persisted in Block 10, where the introduction of new sequences did not revert the established pattern. ANOVA revealed significant group differences across all axes again, see Figure 6 (Hurst Acceleration X: $F(1, 4) = 10.26$, $p = .033$; Hurst Acceleration Y: $F(1, 4) = 21.99$, $p = .009$; and Hurst Acceleration Z: $F(1, 4) = 11.03$, $p = .029$).

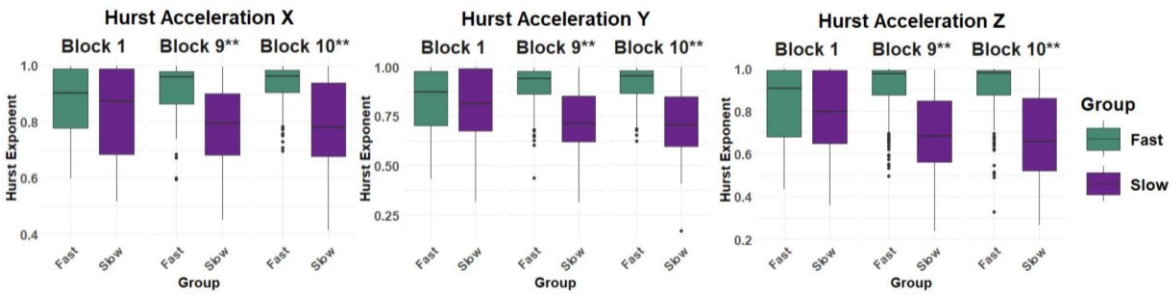

Fig. 6. Comparison of Hurst exponents for 'Fast' vs. 'Slow' performers across blocks 1, 9, and 10 of the Movement Preparation Period. Blocks marked with two asterisks (**) indicate significant differences between groups within those blocks.

4.3.2 Sequence Execution Period

For the sequence execution phase, no significant differences in Hurst exponents were found in the ANOVA between 'Fast' and 'Slow' groups at any block or acceleration axes. The

group differences for all axes of acceleration and over the three blocks 1, 9, and 10 can be seen in Figure 7.

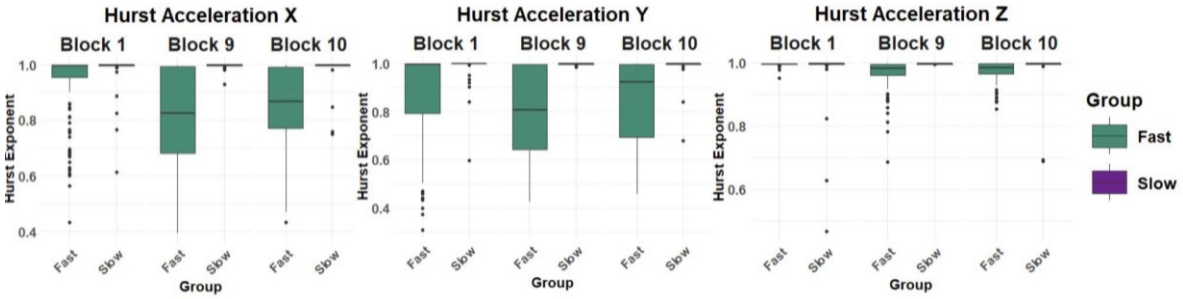

Fig. 7. Comparison of Hurst exponents for 'Fast' vs. 'Slow' performers across blocks 1, 9, and 10 of the Sequence Execution Period.

5. Discussion

This study investigated the COM acceleratory movements in MSL within the trials of participants during different phases of the DS-DSP task, focussing on both sequence execution and movement preparation periods. The main goal was to determine whether fractal properties, as evidenced by Hurst exponents, increase with training and whether they can differentiate between "good" and "bad" performers, as well as their adaptability to new and unfamiliar sequences.

The analyses on the behavioral data indicate that participants demonstrated significant improvements in RT and step accuracies as the experiment progressed. Specifically, the biggest improvements in RT and step accuracy became evident from Block 1 to Block 2 (Figure 3). After the introduction of new and unfamiliar sequences in Block 10, there was a deterioration in sequence performance. Despite this, the RTs and error rates did not revert back to the initial levels observed at the start of the experiment, indicating that learning of the initial sequences had a generalizable effect that participants could at least partly transfer to the new and unfamiliar sequences in Block 10.

5.1 Hypothesis Evaluation

In our study, an increase in Hurst exponents was observed during the movement preparation period for all three axes of acceleration (Figure 4), suggesting clearer fractal scaling properties as participants gained proficiency in the DS-DSP task. This finding aligns with our first hypothesis, which expected that fractal properties would increase across the experimental blocks. Conversely, results from the sequence execution period across all participants showed a long-term decline in Hurst exponents for the X and Y axes of acceleration (Figure 4). This divergence in trends between the movement preparation and sequence execution periods therefore only partially supports our hypothesis. It suggests that while fractal properties may not become more pronounced during active sequence execution, they do appear to increase during the preparatory stages of a trial as participants' familiarity and proficiency with the task grow.

The second hypothesis expected higher Hurst exponents in participants better adapting to unfamiliar sequences introduced in Block 10. This was also partially supported within the movement preparation period. There, the 'Fast' performers displayed significantly higher Hurst exponents across all three axes compared to the 'Slow' performers (Figures 5). This suggests that the 'Fast' group, who adapted more effectively to new sequences, exhibited greater fractal scaling properties during preparatory phases of a trial. Interestingly, such distinctions were not observed during the sequence execution phase, indicating that the predictive value of Hurst exponents for adaptability may be more relevant during the anticipatory stages of task engagement rather than during the active execution of the task.

5.2 Theoretical Implications

5.2.1 Increase in fractal properties for the 'Fast' performers over the course of the DS-DSP task in the Movement Preparation Period

The fact that there are no significant differences in Hurst values between the 'Fast' and 'Slow' performers during Block 1 of the movement preparation phase aligns with the notion that all participants start with a relatively similar cognitive baseline when initially learning the DSP sequences. This could indicate a universal initial phase of motor exploration where the participants are actively exploring motor strategies to cope with the new task. As the trials progress, the increase in Hurst exponents observed only in the 'Fast' performers, suggests a divergence in how these two groups are developing their motor planning strategies over time. The absence of such a pattern in the initial Block 1 might indicate a shift from exploration to more focused exploitation of optimized motor responses in anticipation of the task.

The C-SMB 2.0 framework posits that proficient performers of motor sequences develop strong representations of those sequences within the long-term memory (Verwey, 2023). According to this framework, performers use those stored representations to prepare and execute motor responses. As performers gain proficiency in the task, the central processor becomes more efficient at coordinating the perceptual input of sequences to be performed with the planning and redirecting of output to the motor processors (Verwey, 2023). This increased efficiency of the central processor might also contribute to the observed increases in fractal properties within the 'Fast' participants' COM acceleratory movements during the movement preparation period, which might point to a more complex and adaptable motor control system.

5.2.2 Decreasing trend in fractal scaling within the Sequence Execution Period

The analysis across all participants for the sequence execution period indicated a general decrease in Hurst exponents for the acceleration X and Y axis over time (Figure 4). While ANOVA did not reveal statistically significant differences between the 'Fast' and 'Slow' groups across Blocks 1, 9, and 10, the box plots displayed in Figure 7 suggest a much wider range of Hurst exponents within the 'Fast' group. Interestingly, the participants

belonging to the 'Slow' group, all showed very consistently high Hurst exponents, indicative of fractal scaling, across all acceleration axes and blocks (see Figure A1 of the appendix). The statistically non-significant results from the ANOVA might be attributed to the fact that this same pattern was also present for one 'Fast' performer (Subject 28). The presence of consistently high Hurst exponents across both 'Slow' performers and at least one 'Fast' performer suggests that Hurst exponents, in isolation, may not effectively differentiate between higher and lower proficiency in performers within the sequence execution period.

5.3 Participant-Specific Observations

However, an interesting observation arises when examining the trajectory of Hurst exponents across the blocks of the experiment for the two fastest performers, Subjects 6 and 15 (the red and blue trajectories in Figure A1). Unlike the general trend of consistent fractal scaling in other participants, these subjects exhibited much lower and more varied Hurst exponents for the X and Y axes during sequence execution. Subject 6 already displays this trend from the onset of Block 1, whereas Subject 15 initially had high and consistent Hurst exponents, similar to the other participants. However, as the experiment progresses, Subject 15's pattern begins to shift and align more closely with Subject 6's. The Hurst exponents for the X and Y axes begin to decrease and vary more. This trend of decreasing Hurst exponents in the X and Y axes seen in Subjects 6 and 15 aligns with the general long-term decrease observed across all participants in these axes (Figure 4).

Fractal scaling properties in human movement time series have been shown to emerge more clearly in instances where "constant enactment of control" when performing the movement is necessary (Likens et al., 2015). Furthermore, Ducharme & Van Emmerik (2018) propose that true fractal scaling might be metabolically expensive and that's why we only find scaling exponents around 0.75 in normal unperturbed walking at preferred walking speed, while it is closer to 1 if participants are instructed to walk at faster or slower than

preferred walking speeds. The same has been found for deviations from preferred running speed (Wilson & Likens, 2023). This insight could also explain why higher Hurst exponents differentiate expert slack-liners from novices in the study by Kodama et al. (2023), where constant control and adaptation in acceleratory movements are necessary to maintain balance.

In the context of the DS-DSP task, the transition from higher to lower Hurst exponents in the X and Y axes could reflect a shift from an initial mode of high control to a more automated sequence execution. This pattern suggests a shift from exploration, characterized by high fractal complexity within the motor output as participants search for optimal strategies, to exploitation, where a stable, efficient strategy has been established and is now executed with reduced fractal complexity and metabolic cost. In the language of dynamical systems theory, this observation indicates an attractor the system has settled on, which now minimizes energy use and surprise.

From the standpoint of the C-SMB 2.0, this observed trend among the fastest two performers may reflect a mode of sequence execution that is characterized by a decreased involvement of the central processor. This transition is detailed particularly in the autonomous mode of skill development described by the framework (Verwey, 2023). This stage highlights a transition where extensive practice leads to motor sequences operating independently from central cognitive processes, facilitated by established associations across various processing levels, allowing for autonomous execution by motor processors (Verwey, 2023). Interestingly, Subject 6 demonstrated an exceptionally fast RT from the very beginning of the experiment already (Figure A2 in the appendix). The initial low and varied Hurst exponents in the X and Y axes, coupled with significantly faster RTs compared to other participants, suggest that Subject 6 may have already been operating in an autonomous mode early on, possibly due to prior experience with other motor sequential behavior. In contrast, Subject 15 displayed a similar pattern of Hurst exponents only in the later stages of the

experiment, which might indicate that Subject 15 transitioned into the autonomous mode as the experiment progressed (Figure A1).

As the experiment introduced new and unfamiliar sequences in Block 10, the two participants that had reduced their fractal properties within their motor output previously, now suddenly demonstrate an increase in fractal properties within this block. Subject 6 exhibited an increase within the Acceleration Y axis, and Subject 15 in the X axis, suggesting that their motor control systems now "injected" more variability into their motor output in order to adapt to these new task demands (Figure A1). This increase in fractal properties likely facilitated the exploration of new coordination patterns to optimize performance under these new constraints. These changes highlight the capacity of the motor system to modify control strategies in response to new constraints, aligning with dynamical systems theory which posits that such adaptations represent critical shifts towards new attractors that optimize system behavior under varying conditions.

Another question that remains is why the third fastest participant (Subject 28) has very consistent and high Hurst exponents across all three axes and blocks of the experiment, and does not show the same pattern of reduced fractal properties that we see in Subject 6 and 15. A possible explanation for this might be that Subject 28's performance strategy heavily favored accuracy, which is documented in Table A1 of the Appendix. This suggests that participant 28 might display higher Hurst exponents across all three axes, and does so consistently over all Blocks of the experiment, because this participant likely moved with more precise and conscious attention to also maintain accuracy along with speed. A related explanation as to why certain participants might show consistent fractal scaling across all blocks is that those participants still actively explore the motor space of the task. Especially within the DS-DSP task, performing the sequences offers a lot of degrees of freedom,

because participants have to navigate four locations on the dance mat using two effectors (both legs).

6. Future Directions

Given the findings, further research could explore how instructions or task emphasis (speed vs. accuracy) affect the emergence of fractal properties in the time series during the DS-DSP task. A future iteration of the DS-DSP task could explicitly instruct one group of participants to focus on performing the sequences as fast as possible, while another group of participants is instructed to prioritize accuracy. This approach would allow to test whether emphasizing different aspects of task performance leads to distinctly different fractal properties in COM movements between the groups.

Additionally, another interesting investigation would be to vary the novelty of sequences presented to participants. One group could be tasked with performing the same kind of sequences across all blocks, thereby keeping the constraints constant to facilitate exploitation. In contrast, a second group could receive new and unfamiliar sequences in every block, effectively forcing them to stay in the exploratory phase of learning. This should theoretically maintain higher levels of cognitive and motor control system engagement in the second group, reflected by higher Hurst exponent due to the constant need for adaptive motor planning and execution.

7. Conclusion

This study investigated the performance discriminatory power and relevance of Hurst exponents derived from COM acceleration data in the DS-DSP task. In the movement preparation phase, there seems to be a trend where better performers develop increased or less varied fractal properties in their acceleratory COM movements in anticipation of trial

execution. This suggests that Hurst exponents in this phase could be indicative of an individual's proficiency in preparing for motor execution, which potentially reflects more effective cognitive and motor strategies among better performing participants. However, in the sequence execution phase, Hurst exponents do not seem to predict performance or adaptability, as both the fastest and slowest performers can exhibit consistent fractal scaling across all blocks of the experiment.

This study has discussed the possibility that the reduced and more varied Hurst exponents among some of the fastest performers might indicate a transition to exploitation of consolidated coordination strategies for executing the DS-DSP task. This trajectory of Hurst exponents also suggests how some participants prioritize speed and automatic execution of these learned coordination patterns, which is associated with reduced fractal properties in their acceleratory COM fluctuations. Notably, the participants who displayed a pattern of reduced fractal scaling during the learning phase, showed an increase in fractal properties of their acceleratory movements in Block 10 as a response to the changing task constraints. This increase suggests a re-engagement in exploratory behaviors to optimize coordination under the new task constraints.

Conversely, participants who focus more on accuracy may demonstrate acceleratory COM fluctuations indicative of a motor control system that maintains constant control throughout the sequence execution phase. This control allows for a highly adaptive state, potentially enabling on-the-fly corrections for prior acceleratory movement errors within the sequence execution. Moreover, participants exhibiting consistently high Hurst exponents may be engaging in an exploratory state to optimize their coordination pattern given the high degrees of freedom for performing the DS-DSP task.

If these interpretations hold, Hurst exponents could provide valuable information about the underlying cognitive and motor dynamics that distinguish individual coordination

strategies within complex motor tasks. Such insights could have implications for the field of robotics, where integrating fractal properties into movement algorithms could enhance the adaptability and efficiency of robots in complex, unpredictable environments. In the field of rehabilitation and elderly care, these findings could inform the development of training protocols that incorporate variability in how a task is presented to enhance motor learning and recovery by stimulating adaptive and exploratory coordination variability.

References

Chan, R. W., Wiechmann, E., & Verwey, W. (2022). Motor sequencing learning from dance step: A whole-body version of the discrete sequence production task. https://doi.org/10.31234/osf.io/ypt7n

Davids, K., Glazier, P., Araújo, D., & Bartlett, R. (2003). Movement systems as dynamical systems. *Sports Medicine*, *33*(4), 245-260. https://doi.org/10.2165/00007256-200333040-00001

Dhawale, A. K., Smith, M. A., & Ölveczky, B. P. (2017). The Role of Variability in Motor Learning. *Annual Review of Neuroscience*, *40*, 479-498. https://doi.org/10.1146/annurev-neuro-072116-031548

Diniz, A., Wijnants, M. L., Torre, K., Barreiros, J., Crato, N., Bosman, A. M., Hasselman, F., Cox, R. F., Van Orden, G. C., & Delignières, D. (2011). Contemporary theories of 1/f noise in motor control. *Human Movement Science*, *30*(5), 889-905. https://doi.org/10.1016/j.humov.2010.07.006

Ducharme, S. W., & Van Emmerik, R. E. (2018). Fractal dynamics, variability, and coordination in human locomotion. *Kinesiology Review*, *7*(1), 26-35. https://doi.org/10.1123/kr.2017-0054

Friston, K. (2010). The free-energy principle: A unified brain theory? *Nature Reviews Neuroscience*, *11*(2), 127-138. https://doi.org/10.1038/nrn2787

Goldberger, A. L., Moody, G. B., & Costa, M. D. (2012, April 17). *Variability vs. Complexity*. PhysioNet. Retrieved June 11, 2024, from https://archive.physionet.org/tutorials/cv/

Hart, S. G., & Staveland, L. E. (1988). Development of NASA-TLX (Task load index): Results of empirical and theoretical research. *Advances in Psychology*, 139-183. https://doi.org/10.1016/s0166-4115(08)62386-9

Hausdorff, J. M. (2005). Gait variability: Methods, modeling and meaning. *Journal of NeuroEngineering and Rehabilitation*, *2*(1). https://doi.org/10.1186/1743-0003-2-19

Kodama, K., Yamagiwa, H., & Yasuda, K. (2023). Fractal Dynamics in a Whole-Body Dynamic Balance Sport, Slacklining: A Comparison of Novices and Experts. *Nonlinear Dynamics, Psychology, and Life Sciences*, *27*(1), 15-28. PMID: 36522297

Likens, A. D., Fine, J. M., Amazeen, E. L., & Amazeen, P. G. (2015). Experimental control of scaling behavior: What is not fractal? *Experimental Brain Research*, *233*(10), 2813-2821. https://doi.org/10.1007/s00221-015-4351-4

Likens, A. D., Mangalam, M., Wong, A. Y., Charles, A. C., & Mills, C. (2023). Better than DFA? A Bayesian Method for Estimating the Hurst Exponent in Behavioral Sciences. *ArXiv*. arXiv:2301.11262v1

Mangalam, M., Wilson, T., Sommerfeld, J., & Likens, A. D. (2023). Optimizing a Bayesian method for estimating the Hurst exponent in behavioral sciences. *ArXiv*. arXiv:2301.12064v1

Newell, K. M., & Vaillancourt, D. E. (2001). Dimensional change in motor learning. *Human Movement Science*, *20*(4-5), 695-715. https://doi.org/10.1016/s0167-9457(01)00073-2

Nourrit-Lucas, D., Tossa, A. O., Zélic, G., & Delignières, D. (2014). Learning, motor skill, and long-range correlations. *Journal of Motor Behavior*, *47*(3), 182-189. https://doi.org/10.1080/00222895.2014.967655

Shmuelof, L., Krakauer, J. W., & Mazzoni, P. (2012). How is a motor skill learned? Change and invariance at the levels of task success and trajectory control. *Journal of Neurophysiology*, *108*(2), 578-594. https://doi.org/10.1152/jn.00856.2011

Sigmundsson, H., Trana, L., Polman, R., & Haga, M. (2017). What is trained develops! Theoretical perspective on skill learning. *Sports*, *5*(2), 38. https://doi.org/10.3390/sports5020038

Stergiou, N., & Decker, L. M. (2011). Human movement variability, nonlinear dynamics, and pathology: Is there a connection? *Human Movement Science*, *30*(5), 869-888. https://doi.org/10.1016/j.humov.2011.06.002

Sternad, D. (2018). It's not (only) the mean that matters: Variability, noise and exploration in skill learning. *Current Opinion in Behavioral Sciences*, *20*, 183-195. https://doi.org/10.1016/j.cobeha.2018.01.004

Verwey, W. B. (2023). C-SMB 2.0: Integrating over 25 years of motor sequencing research with the discrete sequence production task. *Psychonomic Bulletin & Review*. https://doi.org/10.3758/s13423-023-02377-0

Wijnants, M. L. (2014). A review of theoretical perspectives in cognitive science on the presence of 1/f scaling in coordinated physiological and cognitive processes. *Journal of Nonlinear Dynamics*, *2014*, 1-17. https://doi.org/10.1155/2014/962043

Wijnants, M. L., Bosman, A. M., Hasselmann, F., Cox, R. F., & Van Orden, G. C. (2009). 1/f scaling in movement time changes with practice in precision aiming. *Nonlinear Dynamics, Psychology, and Life Sciences*, *13*(1), 79-98. PMID: 19061546

Wilson, C., Simpson, S. E., Van Emmerik, R. E., & Hamill, J. (2008). Coordination variability and skill development in expert triple jumpers. *Sports Biomechanics*, *7*(1), 2-9. https://doi.org/10.1080/14763140701682983

Wilson, T. J., & Likens, A. D. (2023). Running gait produces long range correlations: A systematic review. *Gait & Posture*, *102*, 171-179. https://doi.org/10.1016/j.gaitpost.2023.04.001

Zhou, J., Habtemariam, D., Iloputaife, I., Lipsitz, L. A., & Manor, B. (2017). The complexity of standing postural sway associates with future falls in community-dwelling older adults: The mobilize Boston study. *Scientific Reports*, *7*(1). https://doi.org/10.1038/s41598-017-03422-4

Appendix A

Fig. A1. Trajectory of Mean Hurst Exponents for the Fastest and Slowest Performers in the X and Y Axes During the Execution Period. This figure displays the changes in Hurst exponents across ten blocks for participants identified as the three fastest and three slowest performers in Block 10. The gray shaded ribbons represent the standard error of the mean, indicating the varying range in Hurst exponents across trials within each block. Notably, the wider ribbons for participants 6 (light blue line) and 15 (red line) suggest lower and more varied Hurst exponents from trial-to-trial.

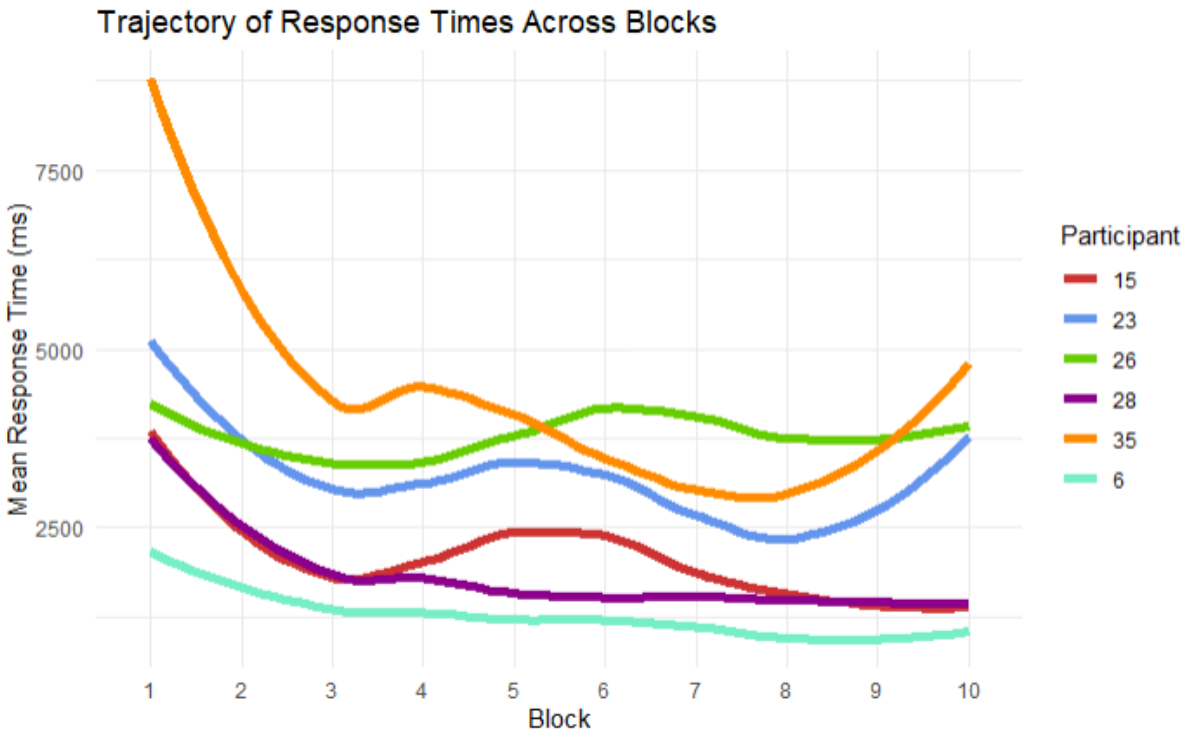

Fig. A2. Learning curve trajectory of Response Times of the Subjects of Analysis Across Blocks. Subject 6 is considerably faster compared to the other participants from the onset of the experiment.

Table A1

Trial Accuracy of the Participants in the 'Fast' Group over All Blocks

Block	Fast		
	Subject 6	Subject 15	Subject 28
1	87.5%	77.08%	97.92%
2	79.17%	89.58%	100%
3	79.17%	89.58%	95.83%
4	85.42%	95.83%	97.92%
5	81.25%	83.33%	97.92%
6	81.25%	85.42%	95.83%
7	87.5%	81.25%	91.67%
8	85.42%	85.42%	97.92%
9	87.50%	83.33%	95.83%
10	87.50%	95.83%	89.58%

Appendix B: Scripts for Data Analysis

B1. Behavioral Analysis Script

This script details the analysis of response times and step accuracies in the behavioral data obtained through the dance mat inputs.

http://rpubs.com/himarcel/1198971

B2. Preprocessing Xsens Data Scripts

B2.1 Preprocessing Xsens data for Movement Preparation Period

This script details the preprocessing steps for the Xsens data during the movement preparation period.

http://rpubs.com/himarcel/1200719

B2.2 Preprocessing Xsens Data for Sequence Execution Period

This script details the preprocessing steps for the Xsens data during the sequence execution period.

http://rpubs.com/himarcel/1200720

B3. Scripts to obtain the Hurst exponents

This script outlines the process of obtaining the Hurst exponents from the preprocessed time series.

http://rpubs.com/himarcel/1200718

B2. Hurst Exponents Analysis Scripts

This script details the analysis of Hurst exponents executed for both the movement preparation period and the sequence execution period.

http://rpubs.com/himarcel/1198969